Physics of Estuaries and Coastal Seas, Dronkers & Scheffers (eds) © 1998 Balkema, Rotterdam, ISBN 90 5410 965 3

On an oscillator equation for tides in almost enclosed basins of non-uniform depth

Leo R. M. Maas
Netherlands Institute for Sea Research, Texel, Netherlands

ABSTRACT: The essential elements in the derivation of an oscillator equation governing the Helmholtz response of an almost-enclosed tidal basin are given. The restoring term becomes nonlinear when the basin has non-uniform depth. Consequences of this non-linearity are briefly discussed.

INTRODUCTION

An enclosed basin has (eigen) modes which are all characterized by the fact that they necessarily conserve mass. Thus, there will always be a zero-elevation line somewhere in the basin, separating regions with opposite phases (180 degrees phase-difference) and they are therefore referred to as sloshing modes (Fig. 1a).

The sole mode added to this system when the basin communicates with a sea through a narrow strait is the "pumping" or Helmholtz-mode, characterized by a periodic mass-exchange through the strait and spatially-uniform elevation change within the basin, see Fig. 1b. This mode occurs when the basin is both deep, so that the flow and therefore frictional effects within the basin are of negligible strength, and short, so that the tidal wave can cross the basin almost instantaneously (LeBlond and Mysak 1978; Mei 1989). As such, this mode may govern the response of (constricted) fjords, although it may also play a contributing role in shallower basins.

When such a basin has vertical side walls it responds linearly to a change in volume transport through the entrance (Fig. 1c); a change that may be either due to natural variability in the tides (e.g. the fortnightly cycle), or to wind effects. The elevation within this linear Helmholtz resonator, in response to a sinusoidal elevation-change in the connecting sea, may thus change amplitude, e.g. due to resonant effects, and phase, due to frictional effects, but will remain sinusoidal in time. Therefore, when the observed basin elevation is not simply a delayed and stretched version of the tide at open sea this points at nonlinear effects. For example, tidal elevations in the Wadden Sea — a complex of tidal basins, seperated by tidal flats and water sheds — (see Fig. 2a) are deformed when compared with tides in the connecting North Sea. Although the tide in these shallow, frictional basins is not of pure Helmholtz-type, maximum delay times amount only to about an hour, much less than a half tidal period which would go with pure sloshing modes, which makes the idealisation to a pure Helmholtz basin of some interest. Within the basin nonlinear bottom-friction and nonlinear advection together with bottom-friction in combination with variations in depth will leads to tidally-rectified, residual current patterns (Zimmerman 1980; Ridderinkhof 1988), but nonlinear behaviour of the Helmholtz mode proper (with its feeble basin flow) is more likely due to nonlinear bottom-friction in the connecting channel (see Zimmerman 1992). Green (1992) suggested that a nonlinear response may also simply be due to the fact that the side walls are not vertical, see Fig. 1d. In here we want to focus just on the essentials of this nonlinear restoring mechanism, both conceptually (Fig. 1), as well as in its derivation. We will also briefly address the consequences of the nonlinearity for the tidal elevations within the basin. A more detailed account of this can be found in Maas (1997), hereafter referred to as *M*.

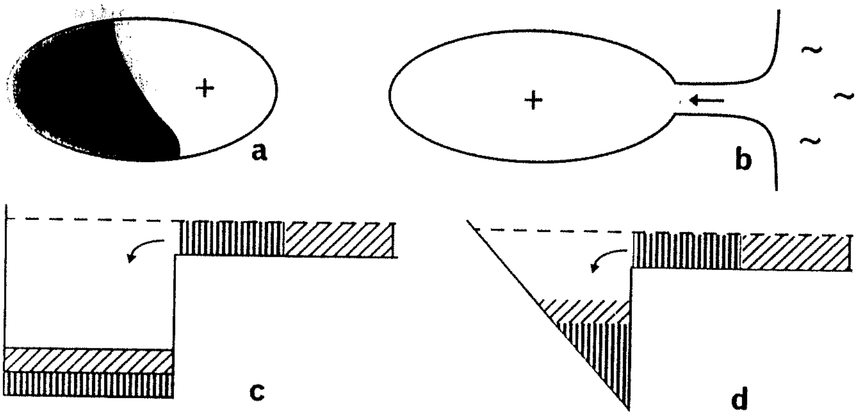

Figure 1: (a) Schematic top view of oscillation in closed basin. Signs indicate positive or negative elevations. (b) Same as (a) but for an almost enclosed basin, showing that water-level displacements can be single-signed. (c) Side-view of a basin with vertical side walls (left) and channel which connects to an open sea (right), showing that equal amounts of subsequently entering packets of fluid induce equal vertical displacements. The basin thus responds linearly to an influx of water. (d) Same as (c) but for a basin with sloping side wall, showing that the vertical displacements induced by equal packets of fluid is now different and depends on the height of the water present when the packet initially flows in. The response of the basin is thus nonlinear. It is relevant to monitor the elevation of the fluid within the basin, because its difference with the tidal height at open sea is driving the flow through the connecting strait.

The relevance of this model in explaining observed tidal characteristics of real bay-inlet systems is something that might be approached, not by rigidly fixing the parameters present in the model, but rather by comparing the particular phenomena that are due to the nonlinear nature of the restoring mechanism with those found in nature. We can here pursue this goal only to a very limited extent, as emphasis will be on the modelling part.

1. DERIVATION OF OSCILLATOR EQUATION

Because of the spatial uniformity of the Helmholtz mode the state of the tide within the estuary can be characterized by a single state-variable: the excess volume $V(t)$ (volume of water relative to mean water level). Its evolution is due to an influx of water, non-dimensionally given as

$$\frac{dV}{dt} = -u, \qquad (1)$$

where u is the strength of the current in the entrance channel (which, as its vertical, cross-sectional area, A_e, is assumed to be spatially uniform). The minus sign at the right hand side of this expression is conventional as the strait direction is defined to be positive towards the open sea. Volume is scaled with horizontal basin area at mean sea level, A_o, multiplied with maximum depth H, and mass flux is scaled by flow-strength multiplied by A_e. Neglecting for the moment nonlinear advective and frictional effects, the flow through the strait is driven by the pressure difference between entrance and exit:

$$\frac{du}{dt} = \zeta - \zeta_e, \qquad (2)$$

where ζ is the spatially uniform elevation within the basin and $\zeta_e(t) = F\cos ft$ is a nondimensional external tide of amplitude F and frequency f. This frequency is nondimensionalized by the Helmholtz-frequency

$$\sigma_H = \left(\frac{gA_e}{A_o L}\right)^{1/2}, \qquad (3)$$

where L is the length of the entrance channel and g the acceleration of gravity. The evolution equations (1) & (2) complete the nonlinear, second-order, oscillator equation once we supply the functional relationship between elevation ζ and volume V. This excess volume $V(t)$ is, by definition, given by the hypsometry of the basin (Boon and Byrne

1981), the basin's area $A(z)$ integrated over depth, from mean water level ($z = 0$) to the free surface ($z = \zeta$):

$$V = \int_o^\zeta A(z)dz. \tag{4}$$

Combining (1) and (2), and adding the omitted nonlinear advection and damping terms, we obtain the following nonlinear, ordinary differential equation, describing the evolution of the dimensionless excess-volume V:

$$\frac{d^2V}{dt^2} + \zeta(V) = F\cos ft - c\frac{dV}{dt} - \gamma\left|\frac{dV}{dt}\right|\frac{dV}{dt} \tag{5}$$

This is a finite-amplitude, forced and damped extension of Green's (1992) model. Mehta and Özsoy (1978) derive a similar lumped-parameter model but apply it to a basin whose cross-sectional area $A(z)$ is constant with height. In particular Eq. (1) then takes the form

$$A_o d\zeta / dt = -uA_e, \tag{6}$$

where all terms are, for this moment, dimensional. Van de Kreeke (1988) and DiLorenzo (1988) pragmatically adopted (6), rather than (1), to apply also to cases where both basin area A_0 as well as cross-sectional entrance area A_e were considered to possess an (empirically determined) time-dependence, so that the restoring term in (5) was replaced by a linear term (albeit with a time-dependent coefficient). Eq. (1) shows this to be unnecessary, as the nonlinear restoring term $\zeta(V)$ is determined by the actual hypsometry and the basin area $A_0(t)$ should thus not be independently prescribed. Following Green (1992), for didactical purposes, it is assumed here that this function is linear throughout the depth of the basin, $A = 1 + z$, such as may be produced by a linearly sloping side-wall. This assumption implies an elevation-volume relationship of the form

$$\zeta(V) = (1+2V)^{1/2} - 1. \tag{7}$$

This description indicates that the basin is "non-empty" as long as $V > -½$ (the dimensionless volume of the basin at rest equals ½). At the right-hand side of (5) we find forcing, and linear and nonlinear friction terms. The forcing represents the "external" tide, characterized by its nondimensional volume-flux and tidal frequency. Linear damping ($\propto c$) is due to seaward radiation of gravity waves (Garrett 1975). Nonlinear damping ($\propto \gamma$) is both due to bottom frictional drag in the connecting strait (Zimmerman 1992), as well as form drag, i.e. an asymmetry of in- and out-flow (Stommel and Farmer 1953). For more details, see *M*.

As the effects of nonlinear damping on basin-tides has been discussed in Mehta and Özsoy (1978), van der Kreeke (1988) and DiLorenzo (1988), and of both linear and nonlinear damping in Zimmerman (1992), these will not be discussed per se. Rather we will put emphasis on the effects of the nonlinear restoring term, although we may remark at the outset that the features to be discussed have been obtained with either of the damping mechanism independently present (as well as in combination).

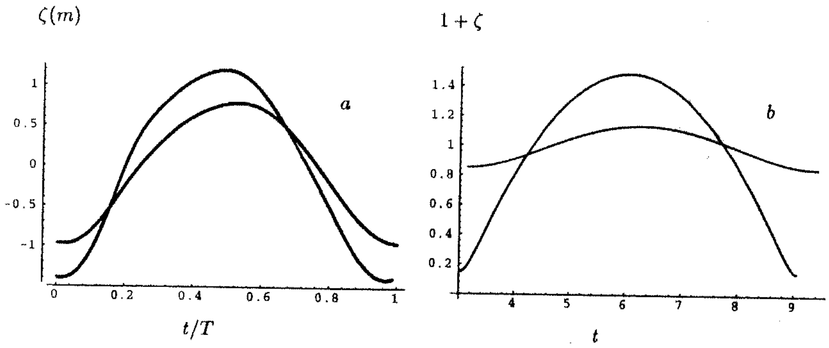

Figure 2: (a) Average spring and neap tidal elevation over one tidal period (T), as observed by Rijkswaterstaat in Lauwersoog at the end of Zoutkamperlaag, a basin in the Dutch Wadden Sea. (b) Free response of the occupied area $A = 1 + \zeta$, related to the excess-volume by $V = (A^2 - 1)/2$, as given by the analytical solutions of the unforced and inviscid evolution equation for V, for initial conditions varying from linear to (large amplitude) fully nonlinear.

2. SOLUTIONS OF OSCILLATOR EQUATION

Without forcing and friction Eq. (5), with (7), can be solved analytically and yields a parametric dependence of volume on time in terms of Jacobian elliptic functions and elliptic integrals (see M). Since, given the same flux of water through the entrance, it takes more time to change the water level when the water is already high (and the occupied area thus large) than when the water is low (and the occupied area small), Fig. 1d, a typical nonlinear response within the estuary consists of sea-level elevations that are "coupled parabola's": long-lasting "highs" versus brief "lows" (see Fig. 2b), not unlike the observed spring-tide elevation in Fig. 2a. Note that the period of the free response (Fig. 2b) drops from 2π to 6 when the nonlinearity increases, in accordance with Green's (1992) perturbative result. A change of the free oscillation period in response to a change in its amplitude is a common feature of nonlinear oscillators (Nayfeh and Mook 1979). It is unusual though, that such a change occurs over a range as small as found here. However, a similar decrease in the basin's observed period in response to the external tide, should therefore not necessarily be a coincidence. (See the weakly discernable difference in time-span between two successive low waters in Fig. 2a, comparing neap and spring tide).

Although the similarity between Figs. 2a and 2b suggests that the response of the forced and damped nonlinear oscillator is perhaps dominated by the free response, in reality, tidal forcing and friction can clearly not be neglected. Numerical integration has therefore been employed to investigate these effects and suggests that several new features may arise. The first two cases discussed below will only add forcing, while, in the last case, also friction is incorporated.

First, for fixed forcing (frequency and amplitude of the external tide), the amplitude of the tidal oscillation within the basin may be varying on a long timescale when the forcing frequency is near-resonance (see Figs 3a,b). This can be explained as follows. Tidal levels are increasing due to the near-resonancy of the basin. However, the eigen-frequency of the basin is now a function of the amplitude and thus changes (natural detuning). As a consequence, the system is brought out-of-resonance and the tidal amplitude drops, from which point the cycle starts again.

Second, there is a tiny region in parameter space for which numerical calculations of the forced, nonlinear Helmholtz oscillator suggest the solutions to be chaotic (see Fig. 3c). This leads to the counterintuitive but intriguing suggestion that one may occasionally expect to observe "chaotic tides": an expression that, in view of the extreme regularity of the tidal forces, might at first look be held as a contradiction in terms!

That tides in estuaries can at certain places be haotic is, however, strongly suggested by the observations of Golmen et al. (1994), see Fig. 4, who, in a fjord in Norway, observed persistent "irregular" sea level and, in particular, current modulations of about 45 minutes period, superposed on the tide. The geometry of the fjord seems to admit the presence of the Helmholtz mode. In contrast to Golmen et al.'s (1994) observation, the Helmholtz period, estimated on the basis of (3), seems to match the observed period. To what extent the "chaos" in their tidal observations can be explained by the above

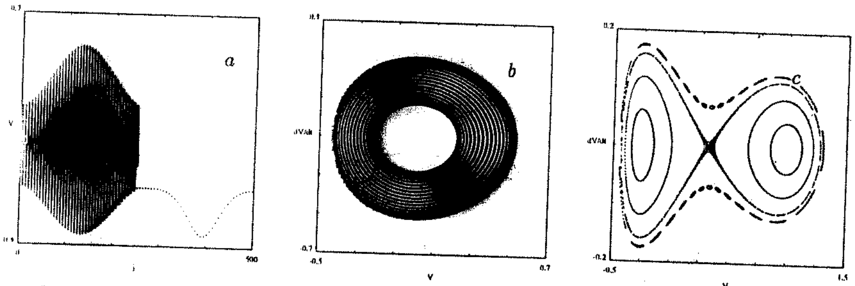

Figure 3: (a) Numerical integration (up to $t = 250$) of the inviscid, forced evolution equation for the excess volume V, demonstrating resonant growth, natural detuning and subsequent decay for $F = 0.01$ and $f = 1$, as given by V versus time t for $V(0) = 0.2$, $dV/dt\ (0) = -0.2$. The dotted curve gives a "stroboscopic plot", as it displays the volume (up to $t = 500$) at times that the external tide is at a minimum: $ft = (2n + 1)\pi$, where n is integer. (b) Plot of same solution but in a plane spanned by strait velocity dV/dt versus volume V. Superimposed, dotted curve on the left side of this figure, gives stroboscopic plot, as in (a). (c) Stroboscopic plot in dV/dt - V plane for forcing amplitude $F = 0.6$ and frequency $f = 1.92$. Four orbits are given in each). which "traces of chaos" are evident in the erratic central orbit (the two inner "orbits" consist of a left and right segment

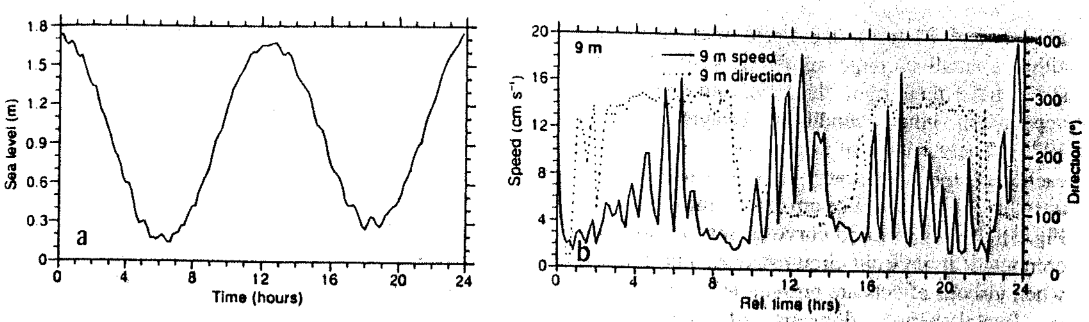

Figure 4: Irregular observed sea level (a) and current (b) observations versus time in Moldefjord, Norway (from Golmen et al. 1994).

(inviscid!) mechanism is unclear as yet, in particular so as the chaos in the theoretical model does not, in general, seem to survive the addition of friction. The loss of chaos under the addition of damping is quite common for perturbed Hamiltonian systems. To specify under what conditions the chaos survives (and thus may perhaps be relevant to the fjord-observations) is currently being investigated.

Third, if, more realistically, we do include friction, direct integration of the system indicates that it settles down into a stationary state (a response curve, $V(t)$, of particular amplitude $\hat{V}$, phase and shape), which is usually independent of initial conditions. The temporal shape of these stationary states may include (but can also be more complex than) the free mode given in Fig. 2b, for instance exhibit an intermediate minimum/maximum within one period, while it may also feature asymmetric profiles, of relevance for net sediment transport. However, the amplitude response curve — giving the amplitude of a stationary state as a function of forcing frequency — need not always indicate that there is a unique state as it may sometimes exhibit multivaluedness for systems close to resonance, see Fig. 5 and M. This means that, for the same values of the "parameters of the system" (characterizing

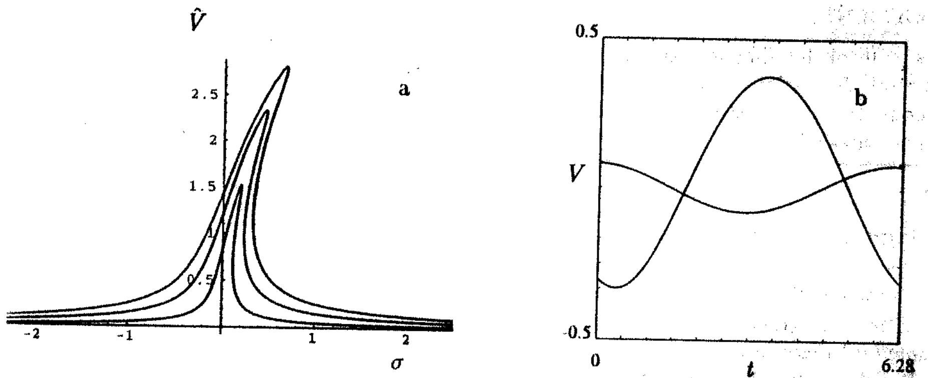

Figure 5: (a) Amplitude response $\hat{V}$ -curves against detuning frequency σ. The detuning frequency gives (an amplified view of) the mismatch between the actual ($f = 1 + \varepsilon^2\sigma$) and the resonance frequency (1). Here $\varepsilon << 1$ is the detuning parameter. For cases of near-resonant forcing, $f \approx 1$ and $\sigma = O(1)$, this curve has "bent resonance horns" and therefore multiple equilibria. It exhibits an increased response with F increasing from $F = 0.1$ to 0.3 and 0.5, for frictional parameters $c = \gamma = 0.01$. Near $\sigma \approx 0.5$ three equilibria are found, the smallest and largest of which are stable. The bent towards the right classifies this oscillator as a "hardening spring" (Nayfeh and Mook 1979). (b) Time evolution of volume within basin in the two equilibrium states. The low (high) range tide is approximately in (out of) phase with the external tidal elevation $F\cos(ft)$.

forcing and friction), the basin may respond with either a small or large amplitude oscillation, which states have their own "basin of attraction" that do depend on initial conditions (Nayfeh and Mook 1979). These basins of attraction are separated from eachother by a separatrix that emanates from the unstable third equilibrium (the middlest one in Fig. 5). This is a closed curve (whose location can be computed) in inviscid circumstances, but it winds out when viscous effects are present, and may indeed lead to fractal-shaped domains of attraction. The implication of the existence of muliple equilibria is that one of the two stable modes may cease to exist for slightly changing parameter values. Thus, when this parameter alters slowly, and passes a threshold — the range of frequencies for which three equilibria exist — it may force the system to rapidly change its state of oscillation to the only remaining state, thereby creating a strong response. Changes like these may perhaps be triggered by changes in mean sea-level. With reference to observations in the Strangford Lough, Northern-Ireland, it has been suggested by Dr. G. Savidge of the Queen's University of Belfast (personal communication) that evidence of such rapid changes in estuarine tidal amplitudes may be hidden in observed sedimentological zonation-patterns. This abrupt drop in tidal range may ultimately form the most dramatic demonstration that a tidal estuary with sloping bottom constitutes a nonlinear oscillator.

ACKNOWLEDGEMENTS

The author likes to thank Jef Zimmerman and Arjen Doelman for useful discussions and an unknown referee for his comments on an earlier draft. This is NIOZ contribution number 3207.

REFERENCES

Boon, J.D. & R.J. Byrne 1981. *On basin hypsometry and the morphodynamic response of coastal inlet systems*. Mar. Geol. 40: 27-48.

DiLorenzo, J.L. 1988. *The overtide and filtering response of small inlet/bay systems*. In D.G. Aubrey & L. Weishar (eds), Hydrodynamics and sediment dynamics of tidal inlets: 24-53. New York: Springer.

Garrett, C. 1975. *Tides in gulfs*. Deep-Sea Res. 22: 23-35.

Golmen, L.G., J. Molvaer & J. Magnusson 1994. *Sea level oscillations with super-tidal frequencies in a coastal embayment of western Norway*. Cont. Shelf Res. 14: 1439-1454.

Green, Th. 1992. *Liquid oscillations in a basin with varying surface area*. Phys. Fluids A, 4: 630-632.

LeBlond, P.H. & L.A. Mysak 1978. *Waves in the ocean*. Amsterdam: Elsevier.

Maas, L.R.M. 1997. *On the nonlinear Helmholtz response of almost-enclosed tidal basins with sloping bottoms*. J. Fluid Mech. 361-380.

Mehta, A.J. & E. Özsoy 1978. *Flow dynamics and nearshore transport*. In P. Bruun (ed) Stability of tidal inlets: 83-161. Amsterdam: Elsevier.

Mei, C.C. 1989. *The applied dynamics of ocean surface waves*. Singapore: World Scientific.

Nayfeh, A.H. & D.T. Mook 1979. *Nonlinear oscillations*. New-York: Wiley-Interscience: 704 pp.

Ridderinkhof, H. 1988. *Tidal and residual flows in the western Dutch Wadden Sea 1: Numerical model results*. Neth. J. Sea Res. 22: 1-21

Stommel, H. & H.G. Farmer. 1953, *Control of salinity in an estuary by a transition. J. Mar. Res.* 12: 13-20.

Van de Kreeke, J. 1988. *Hydrodynamics of tidal inlets*. In D.G. Aubrey and L. Weishar (eds), Hydrodynamics and sediment dynamics of tidal inlets: 1-23. New York: Springer.

Zimmerman, J.T.F. 1980. Vorticity transfer by tidal currents. *J. Mar. Res.* 38: 601-630.

Zimmerman, J.T.F. 1992. *On the Lorentz linearization of a nonlinearly damped tidal Helmholtz oscillator*. Proc. Kon. Ned. Akad. v. Wetensch. 95: 127-145.